



Cite this: *Anal. Methods*, 2019, 11, 205

Stable and reproducible nano-electrospray ionization of aqueous solutions and untreated biological samples using ion current limitation combined with polarity reversing†

Md. Matiur Rahman * and Konstantin Chingin 

Owing to its high chemical sensitivity and low sample consumption, nano-electrospray ionization mass spectrometry (nESI-MS) is nowadays widely used in various fields such as chemistry, biology, medicine, pharmaceutical industry, clinical assessment and forensic science. The key analytical limitations of conventional nESI-MS analysis include low stability and poor tip-to-tip reproducibility of analyte signals due to the common clogging of glass capillary tips and the occurrence of electric discharge, especially for the analysis of aqueous solutions. In this study, the nESI current was greatly reduced and the corona discharge was efficiently quenched using a 10 GΩ resistor placed in series between a pulled glass capillary and a high voltage power supply. Additionally, polarity reversing was applied for the *in situ* salt removal and higher signal intensity than in conventional nESI. Furthermore, by closing the back side of the pulled glass capillary during the analysis the sample flow rate could be reduced down to *ca.* 1 nL min⁻¹. This combined approach allows the analysis of various aqueous solutions and untreated biological samples without tip clogging and electric discharge both in positive and negative modes with enhanced chemical sensitivity, high signal durability (up to several hours per sample) and excellent tip-to-tip reproducibility (80–90%). We believe that the proposed approach may solve many current problems and significantly advance nESI mass spectrometry in the very near future.

Received 2nd October 2018
Accepted 26th November 2018

DOI: 10.1039/c8ay02159g

rsc.li/methods

1. Introduction

Nano-electrospray ionization (nESI) is the advancement of traditional electrospray ionization (ESI), which has become widely used in many fields of mass spectrometry analysis.^{1–3} The main advantages of nESI over traditional ESI include low sample consumption⁴ (few μL), low flow rate (10–20 nL min⁻¹), and higher tolerance to ion suppression and matrix effects.^{5–7} There are two principal modes of nESI-MS analysis: online and offline. The online nESI is simple in assembly and can be directly interfaced with LC for non-interrupted operation.⁸ Unfortunately, online nESI is highly prone to cross-contamination and capillary clogging,⁹ which can strongly interfere with analyte detection and quantitation, mainly due to the matrix effects. Due to the evident problems of online nESI, the offline nESI mode is increasingly preferred in research laboratories. In the offline nESI disposable pulled glass capillaries are typically used as emitters.⁴ Unfortunately, the performance of offline nESI is highly sensitive even to minor

changes during the experiment, *e.g.* changes in the emitter geometry,¹⁰ electric current, flow rate, and tip-to-tip variations.¹¹ Other common problems also include arcing and capillary tip breakage, especially when highly conductive aqueous solutions are analyzed.¹¹ Overall, the tip-to-tip reproducibility and sensitivity of nESI analysis cannot be guaranteed even in the hands of an experienced person.^{12–14}

Several strategies have been proposed in order to improve the performance of nESI.^{10,15} In step-voltage nESI, at first a high voltage (4.5–5.6 kV) is applied to the aqueous solution in the capillary for 30 s. The application of high voltage results in high ion current (*ca.* 10 μA) and electric discharge. Then, the voltage is lowered down to 2.4 kV for more sensitive analyte detection.¹⁵ The increased sensitivity of detection in step-voltage nESI has been attributed to the obviation of suppression effects. It is believed that the initial high current allows efficient electrophoretic separation between analyte ions and salt ions within the capillary. However, the exact mechanism of signal enhancement in step-voltage nESI remains not well understood.¹⁵ Bearing similarity to step-voltage nESI, polarity reversing nESI (PR-nESI) has been recently introduced for the obviation of ion suppression during nESI analysis of aqueous solutions.¹⁰ In PR-nESI a negative high voltage (–3.0 kV) is first applied to the pulled glass nanocapillary for six seconds. This

Jiangxi Key Laboratory for Mass Spectrometry and Instrumentation, East China University of Technology, Nanchang 330013, People's Republic of China. E-mail: matiurrahmanbot@yahoo.com; matiurrahman@ecit.cn; Tel: +86-13177870051

† Electronic supplementary information (ESI) available. See DOI: 10.1039/c8ay02159g

step is probably responsible for the discharge-driven electrophoretic separation within the capillary. After this step, the voltage is switched to a positive voltage of lower magnitude (+1.75 kV). While both techniques demonstrate evident increase in analyte signal intensities compared to the conventional nESI, many critical problems of nESI still remain open, in particular poor reproducibility, stability, atmospheric discharge and capillary clogging.

Several approaches have been proposed to quench the atmospheric discharge during the ESI and nESI analysis of aqueous solutions, including the use of high gas pressure in the ionization area,^{16–23} trace amounts of trifluoroethanol,²⁴ pneumatic-assisted ESI like ion spray,²⁵ and electrosonic spray,^{11,26} as well as the use of strongly dielectric nebulizing gases.^{27–29} An alternative yet poorly studied approach to obviate atmospheric discharge demonstrated by some authors is to reduce the electric current in the ESI circuit by placing a high-ohmic resistor in series with the emitter and high voltage power supply.^{30,31}

Inspired by the earlier research, in this study we propose a new nESI approach that combines the idea of polarity switching with the use of high-ohmic (10 G Ω) resistor for current limitation. We demonstrate that while each of these approaches has its own limitations when applied independently, their combination allows synergy in the analytical performance of nESI for aqueous solutions, manifested in the excellent signal reproducibility and durability, high signal intensity, access to higher ionization voltages without electric discharge, *in situ* salt removal, workability in negative ion detection mode and greatly improved cost-efficiency of analysis. Based on the long-term extensive experience with this nESI-MS approach in our laboratory, we strongly believe that it may solve many current problems and significantly advance nESI mass spectrometry in the near future.

2. Experimental

2.1 Mass spectrometer

A Bruker-HCT ion trap mass spectrometer (Bruker Daltonics Inc., Bremen, FreieHansestadt Bremen, Germany) was used for all experiments. The data were recorded in both positive and negative ion detection modes. The experimental parameters for the Bruker-HCT ion trap mass spectrometer were as follows: nitrogen drying gas flow rate, 10 L min⁻¹; capillary temperature, 180 °C; and multipole RF amplitude (V_{p-p}), 300 V. The ion trap mass range was set from 100 to 3000 Th in both positive and negative ion modes. The capillary temperature was optimized and maintained at 150–180 °C. According to our experience with the Bruker-HCT ion trap instrument, the capillary temperature of 150–180 °C allows the highest long-term signal stability and high signal intensity. Therefore, we used this temperature range in our experiments.

2.2 ESI source

Fig. 1 shows the schematic diagram of the nESI ion source used in this study. For simplicity, further we refer to this ion source

as PR-R-nESI, “PR” stands for polarity reversing and “R” for high-ohmic resistor. A pulled glass capillary with a tip i.d. of \sim 1 μ m is produced in-house from a glass capillary (i.d. 0.8 mm, o.d. 1.5 mm) using a micropipette puller (model P-1000, Sutter Instrument Inc., USA). The sample solution (1–5 μ L) is loaded into the pulled glass capillary using a gel loading pipette tip (i.d. 120 μ m). A silver-coated platinum (Pt) wire is inserted directly into the solution from the back side of the capillary. The back side of the nanocapillary is closed with a septum to prevent evaporation of the sample solution. The assembly is fixed in front of a mass spectrometer using a plastic union and Teflon tubing such that the tip of the pulled glass capillary is \sim 3 mm away from the inlet capillary of the mass spectrometer. The back end of the Pt wire is connected to a metal screw. A resistor is placed in series between the screw and a high voltage power supply. In positive ion mode, high voltage is applied in two steps: (1) -3.5 kV for 6 s and (2) $+1.7$ kV for the remaining time of analysis. In negative ion mode, high voltage is applied in three steps: (1) -3.5 kV for 6 s; (2) $+1.7$ kV until a strong positive-ion signal shows up (usually, \sim 30 s); and (3) -1.5 kV for the remaining time of analysis in negative ion mode.

2.3 Sample preparation

Bovine heart cytochrome *c*, horse heart myoglobin, chicken egg lysozyme, bradykinin, MRFA (Met-Arg-Phe-Ala) and leucine enkephalin (YGGFL) were prepared in pure water and then diluted with 0.1% formic acid. All proteins were prepared in water and then diluted in 100 mM NH₄Ac. All chemicals were used without further purification. A 1 μ L sample solution was used for the nanospray analysis. The leaf of *Datura stramonium* was collected directly from a growing plant in Beijing municipality. All fruits were purchased from a local market in Beijing, China, and analyzed without any sample pretreatment. Plant materials were stabbed to \sim 5 mm depth using a Pt wire in order to collect the sample, and the wire was directly inserted into the nanocapillary tip containing \sim 1–2 μ L of aqueous solution for the immediate nESI analysis. This silver-coated Pt wire with an o.d. of \sim 50 μ m was purchased from Ida Tianjin Co. (Tianjin, China). A commercial gel loading tip (epT.I.P.S, Eppendorf, Germany) with an inner diameter of 120 μ m was used for loading the sample onto a pulled glass capillary throughout this study. The deionized water was purchased from Hangzhou

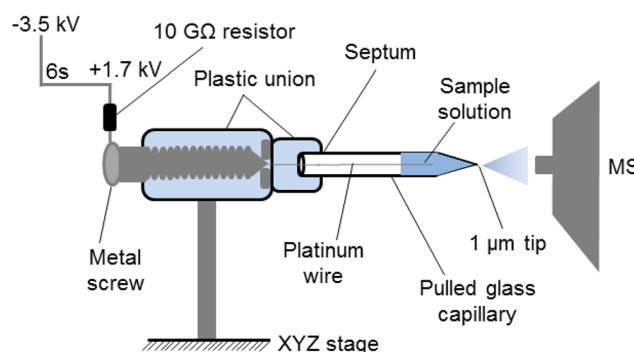


Fig. 1 Schematic diagram of the PR-R-nESI ion source.

Wahaha Group Co., Ltd., China. All samples and methanol were purchased from Sigma Aldrich (St. Louis, MO, USA).

3. Results and discussion

3.1 The effect of maximum time of ion injection

The effect of maximum time of ion injection on the PR-R-nESI ion source is tested using 10^{-5} M cytochrome *c* prepared in 0.1% formic acid aqueous solution. The Bruker-HCT ion trap instrument is operated at different maximum times of ion injection (0.1–50 ms). The ion intensities originating from cytochrome *c* are plotted in Fig. S1.† Every injection time in Fig. S1† has been examined using three measurements. The maximum time of ion injection of 0.7–1 ms is found to provide the highest ion signal intensity. The result agrees with a recent study on the optimal maximum time of ion injection using desorption atmospheric pressure chemical ionization on the same instrument.³² Hence, in all the experiments reported below the ion injection time of 0.7 ms is used.

3.2 The measurement of PR-R-nESI flow rate

The experimental procedure used in this study to estimate the PR-R-nESI flow rate is similar to that for a standard nESI ion source with a capillary tip diameter of *ca.* 1 μm .⁴ For $50 \mu\text{g mL}^{-1}$ MRFA peptide in water with 5% methanol, the average flow rate for PR-R-nESI is $\sim 20 \text{ nL min}^{-1}$ when the backside of the capillary is open. This flow rate is consistent with the flow rates commonly reported for conventional nESI with a capillary tip diameter of *ca.* 1 μm .^{4,33} Interestingly, when the backside of the capillary is closed by a septum during the analysis, the average flow rate for PR-R-nESI using the same sample solution is decreased *ca.* 20 times down to only $\sim 1 \text{ nL min}^{-1}$. The instantaneous flow rate is difficult to measure, but the average flow rate could be estimated by comparing the liquid amount before and after the run. The flow rate in this study is estimated as $\sim 1\text{--}3 \text{ nL min}^{-1}$. At this low flow rate, a 1 μL aqueous sample solution can be analyzed over at least several hours without interruption. Apparently, the decrease in the flow rate when using

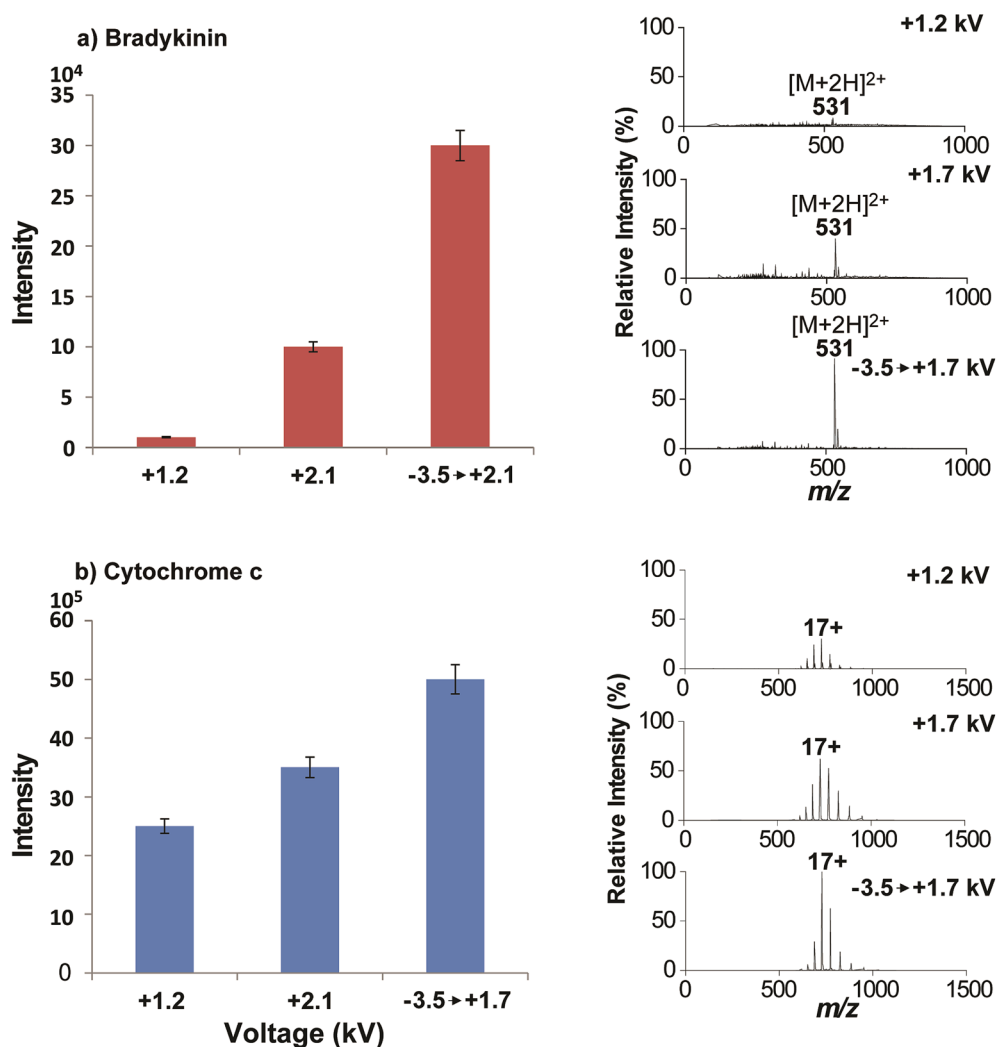


Fig. 2 Comparison of conventional nESI (+1.2 kV and +1.7 kV) with PR-R-nESI (-3.5 kV for 6 s, then +1.7 kV) for the analysis of bradykinin ($1 \mu\text{g mL}^{-1}$) (a) and cytochrome *c* ($120 \mu\text{g mL}^{-1}$) (b) in water with 0.1% formic acid. Three replicate experiments were performed. Other instrumental settings were identical.

the closed capillary is due to the drop in the pressure of head-space gas within the capillary during the analysis (<1 atm). As a result, the gas pressure inside the capillary is lower than the gas pressure outside the capillary, and this difference is responsible for the occurrence of back-pressure force on the solution inside the capillary. The low volatility of water is not sufficient to replenish the gas pressure during the analysis. The possibility of reducing the flow rate down to 1 nL min^{-1} simply by closing the backside of the nESI capillary is indeed a very curious and potentially useful finding, which somehow has been largely overlooked in earlier literature. Indeed, more research is necessary on this matter.

3.3 Comparison between PR-R-nESI and conventional nESI

Water is the most problematic solvent in nESI. Due to its high conductivity, water commonly produces electric discharge,

which can strongly affect the sensitivity and reproducibility of analysis. Therefore, high voltages (>2 kV) are usually avoided during the analysis of aqueous solutions by nESI. The use of PR-R-nESI addresses the problem of electric discharge by using a high-ohmic resistor, which reduces the nESI current (Fig. S2†). Fig. 2 compares the performance of PR-R-nESI and nESI for the analysis of bradykinin ($10 \mu\text{g mL}^{-1}$) and cytochrome *c* ($120 \mu\text{g mL}^{-1}$) prepared in water with 0.1% formic acid. Overall, PR-R-nESI is found to yield stronger ion signal intensity than conventional nESI at different ionizing voltages.

The enhanced detection sensitivity and other advantages of PR-R-nESI over conventional nESI are further demonstrated by comparing the results for the peptide leucine enkaphalin ($1 \mu\text{g mL}^{-1}$ in pure water) and myoglobin ($167 \mu\text{g mL}^{-1}$ in water with 0.1% formic acid), both in positive and negative ion detection modes (Fig. 3). In positive mode, the signal of leucine enkaphalin in conventional nESI-MS alongside the protonated signal

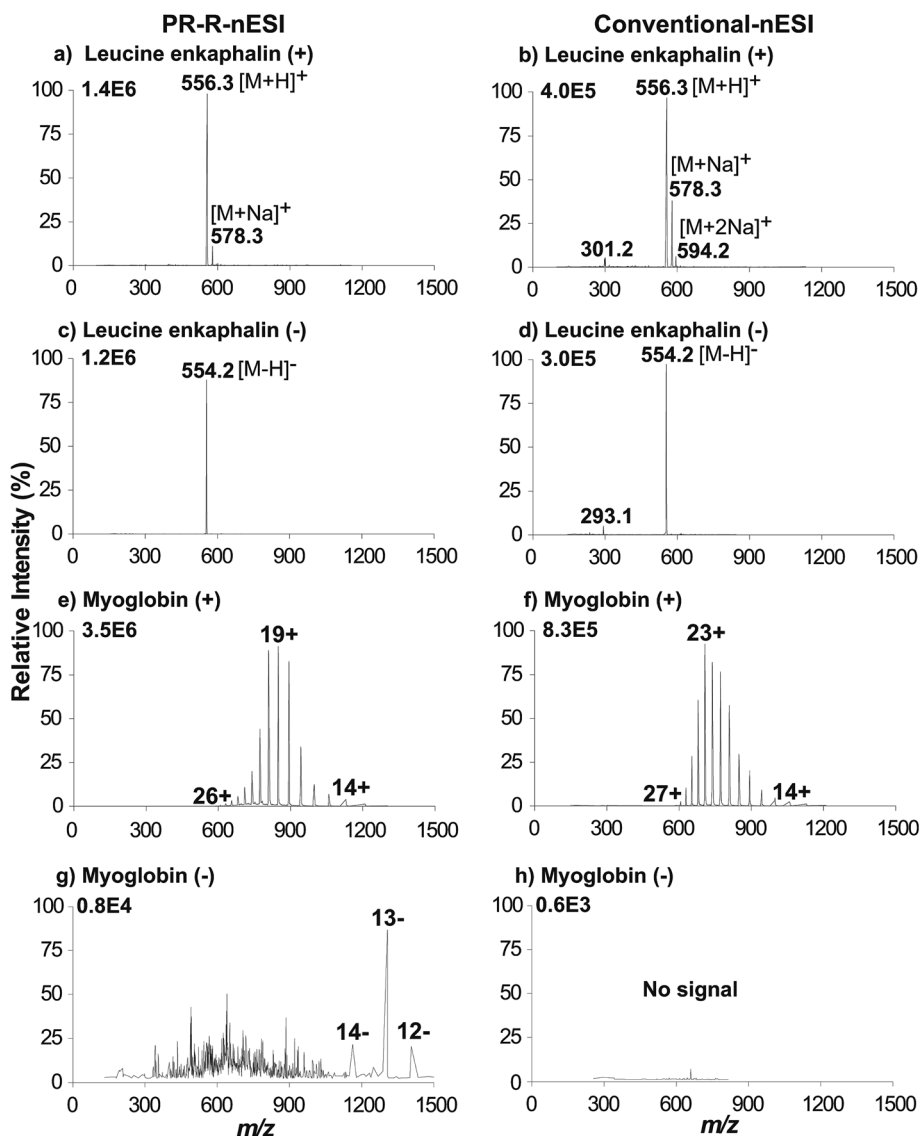


Fig. 3 The comparison between PR-R-nESI-MS (a, c, e and g) and conventional nESI-MS (b, d, f and h) for the analysis of leucine enkaphalin ($1 \mu\text{g mL}^{-1}$) in pure water (a–d) and myoglobin ($167 \mu\text{g mL}^{-1}$) (e–h) in water with 0.1% formic acid in both positive and negative ion modes.

$[M + H]^+$ also shows a considerable contribution of the sodiated adduct $[M + Na]^+$ (Fig. 3b). In contrast, the sodiated adduct is almost absent in PR-R-nESI-MS (Fig. 3a). The desalting effect in PR-R-nESI is most probably related to the electrophoretic separation between the sodium ions and the analyte peptide occurring during the negative high-voltage pulse.¹⁰ The comparison for myoglobin in positive ion mode shows lower charging in PR-R-nESI compared to conventional nESI (Fig. 3e and f). The average charge state is *ca.* 19 in PR-R-nESI while 22 in conventional nESI. The lower degree of charging for myoglobin in PR-R-nESI is probably related to the reduced nESI current due to the use of the 10 G Ω resistor (Fig. S2†). According to our data, the sensitivity of PR-R-nESI at 1 nL min⁻¹ is typically *ca.* 5 times higher than the sensitivity of conventional nESI at 20 nL min⁻¹ (*e.g.*, see Fig. 3e and f). The accurate comparison is complicated due to the alterations in flow rates during the run.

The advantage of PR-R-nESI over conventional nESI is particularly vivid for the analysis in negative ion mode. The nESI analysis in negative mode is generally much more difficult than in positive mode due to the higher vulnerability to electric discharge. This problem greatly affects the sensitivity of detection. Thus, we failed to detect the myoglobin signal from water in negative ion mode using conventional nESI (Fig. 3h). In contrast, PR-R-nESI enables more sensitive and stable analysis in negative ion mode owing to the reduction of electric current (Fig. S2†) and obviation of electric discharge. The comparison for leucine enkephalin also shows considerable sensitivity enhancement in negative mode for PR-R-nESI (Fig. 3c and d).

Of particular importance is that the use of PR-R-nESI efficiently obviates tip clogging and electric discharge and thus enables high tip-to-tip reproducibility. In our hands, the use of conventional nESI resulted in about 50% tip clogging, whereas the use of current-controlled PR-R-nESI reduced the probability

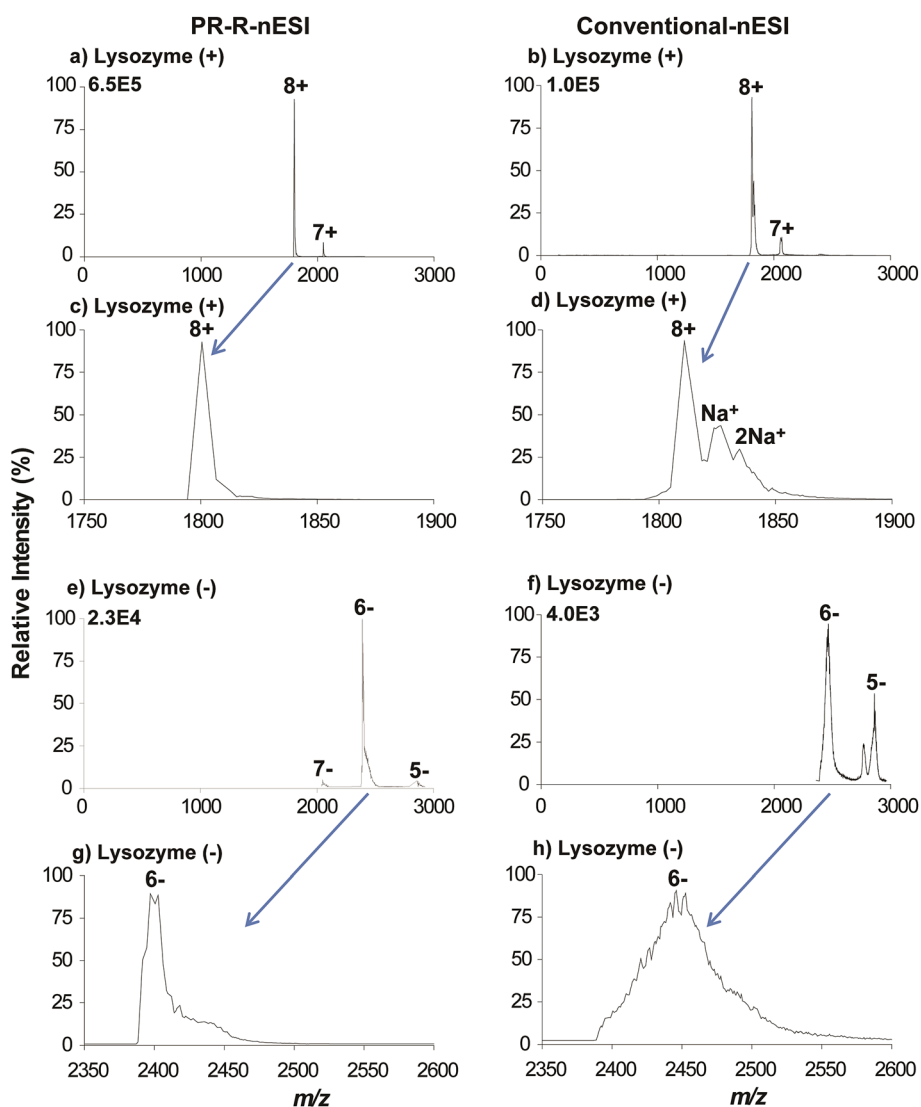


Fig. 4 Comparison of PR-R-nESI (a, c, e and g) and conventional nESI (b, d, f and h) for lysozyme (120 $\mu\text{g mL}^{-1}$) in 100 mM NH_4Ac aqueous solution. The 8^+ charged peak for positive ion mode (b and f) and the 6^- charged peak for negative ion mode (d and h) are amplified to show the signal shape.

of tip clogging to below 10%. The reduced tip clogging in PR-R-nESI is most probably related to the substantially lower nESI current and obviation of arcing and corona discharge even at high ionizing voltages. On average, 80–90% of capillaries yield reproducible signal intensities for the same sample (RSD within 10%) in PR-R-nESI experiments.

3.4 Detection of intact proteins using PR-R-nESI

Fig. 4 compares the performance of conventional nESI and PR-R-nESI for the analysis of lysozyme ($140 \mu\text{g mL}^{-1}$) in 100 mM ammonium acetate (NH_4Ac) aqueous solution. Both in positive and negative ion modes the use of PR-R-nESI yields a *ca.* 6-times increase in ion signal intensity as well as a pronounced desalting effect, resulting in much sharper peak shapes (Fig. 4a, c, e and g). Similar behavior is found for cytochrome *c* and myoglobin ($167 \mu\text{g mL}^{-1}$) in 100 mM aqueous NH_4Ac (Fig. S3†). Apparently, PR-R-nESI is a very promising ionization method

for the analysis of intact proteins. The use of polarity reversing accounts for the desalting effect, while the use of current limitation minimizes ion current in the capillary and enables stable protein analysis in the both ion modes.

3.5 Plant materials analysis

When applied to the analysis of matrix sample solutions and biological samples, conventional nESI using a pulled glass capillary as an emitter severely suffers from clogging. In contrast, PR-R-nESI allows nESI analysis of aqueous solutions and untreated biological samples without clogging and with high tip-to-tip reproducibility. Fig. 5 demonstrates the direct PR-R-nESI analysis of an untreated orange, grape, small orange and potato, which are representative juicy and solid biological samples. First, the pulled glass capillary was loaded with $2 \mu\text{L}$ of solvent ($\text{H}_2\text{O} : \text{CH}_3\text{OH} 95 : 5 \text{ v/v}$) using a gel loading tip. Second, the surface of a biological sample was stabbed by a Pt wire to

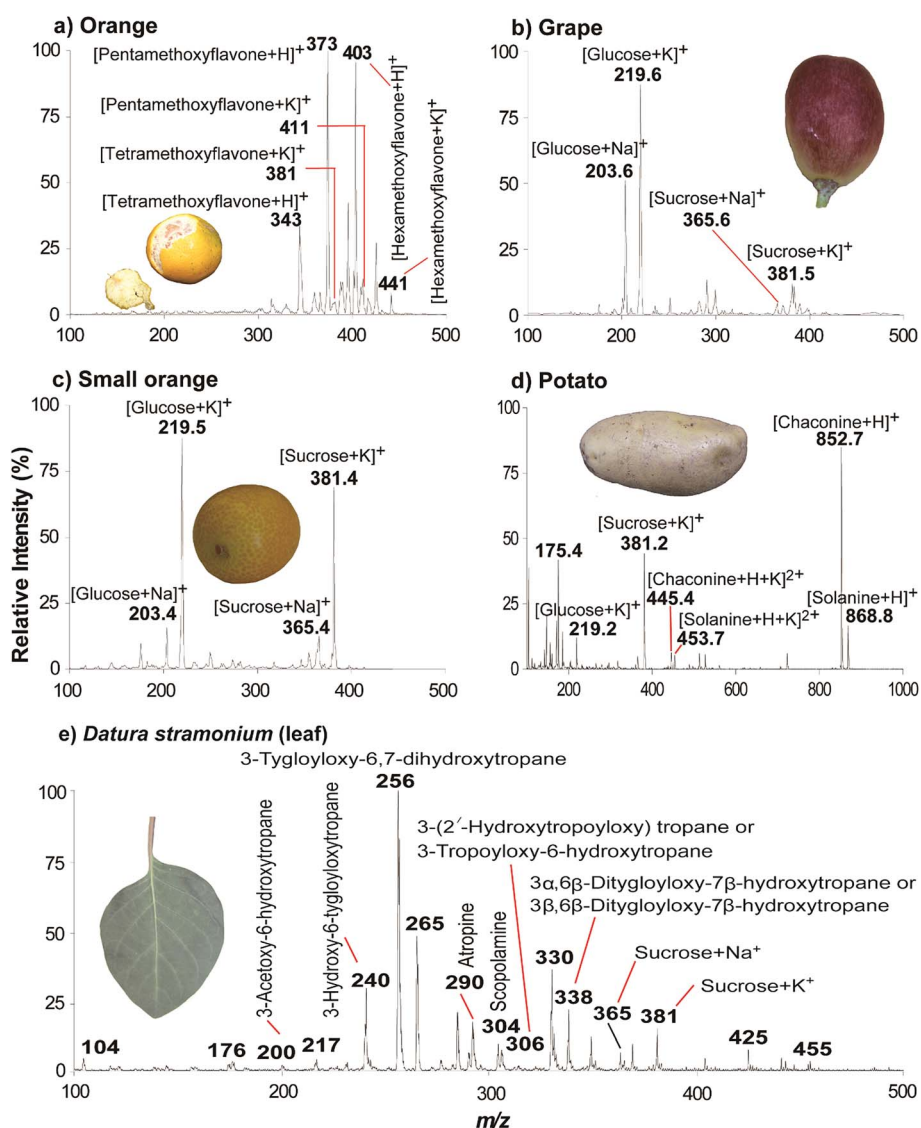


Fig. 5 Direct PR-R-nESI-MS analysis of untreated biological samples: (a) orange, (b) grape, (c) small orange, (d) potato and (e) *Datura stramonium* (leaf).

a depth of ~ 5 mm. Third, the wire was immersed into the spraying capillary and then mounted on the nESI holder in front of a mass spectrometer. Fourth, PR-R-nESI analysis was started. Mass spectra show abundant signals of potassiumated and sodiated glucose, sucrose, protonated flavonoids and alkaloids (Fig. 5). The potassium adduct was more abundant than the sodiated adduct due to the high concentration of potassium in the analyzed samples. Our data are consistent with those obtained by *in vivo* nESI,³⁴ ballpoint ESI³⁵ and DESI.³⁶ This result shows that PR-R-nESI can also be utilized for the direct molecular analysis of untreated biological samples with high chemical sensitivity and without clogging. Potentially, the described mode of nESI analysis can be easily coupled with liquid extraction surface analysis (LESA),^{37,38} which also relies on tip sampling, for the direct analysis of biological samples (tissue analysis, biological fluids, single cell analysis) by a robotic system.

4. Conclusion

In this report, we showed that an integrated nESI approach that combines polarity reversing with current limitation resolves many critical issues of conventional offline nESI analysis using pulled glass capillaries. The use of polarity reversing allows *in situ* desalting and sensitivity enhancement, whereas the use of current limitation greatly alleviates the problem of electric discharge, which is particularly critical for the analysis in negative ion mode. There are two main factors that could possibly be responsible for the increased sensitivity of PR-R-nESI compared to the conventional nESI. The first factor is the low flow rate. The second factor is polarity reversing. Further, both factors are beneficial to avoid tip clogging and ensure high tip-to-tip reproducibility. Interestingly, by closing the back side of the nESI capillary during the experiment, we were able to reduce the sample flow rate down to *ca.* 1 nL min⁻¹. Based on our current experience with PR-R-nESI, we believe that this method greatly alleviates all the major problems of current offline nESI. Moreover, the method extends the application range of nESI towards the direct analysis of concentrated aqueous solutions and untreated biological samples. Indeed, there is substantial room for further improvement to gain even higher sensitivity and lower flow rates (pico electrospray ionization), *e.g.* by using emitters with smaller diameters (60–100 nm). We plan to pursue this goal in near future.

Conflicts of interest

There are no conflicts to declare.

Acknowledgements

This work was supported by the National Natural Science Foundation of China (21475010, 21765001), MOST instrumentation program of China (2012YQ040140-07), State Key Laboratory of Explosion Science and Technology (YBKT16-17, KFJJ13-1Z), Program for Changjiang Scholars and Innovative

Research Team in University (No. IRT_17R20) and 111 Project (No. D17006).

References

- 1 J. Chen, S. Yin, Y. Wu and J. Ouyang, *Anal. Chem.*, 2013, **85**, 1699–1704.
- 2 G. Scherperel, G. E. Reid and R. Waddell Smith, *Anal. Bioanal. Chem.*, 2009, **394**, 2019–2028.
- 3 M. Karas, U. Bahr and T. Dülcks, *Fresenius. J. Anal. Chem.*, 2000, **366**, 669–676.
- 4 M. Wilm and M. Mann, *Anal. Chem.*, 1996, **68**, 1–8.
- 5 A. A. M. Heemskerck, J.-M. Busnel, B. Schoenmaker, R. J. E. Derks, O. Klychnikov, P. J. Hensbergen, A. M. Deelder and O. A. Mayboroda, *Anal. Chem.*, 2012, **84**, 4552–4559.
- 6 G. T. T. Gibson, S. M. Mugo and R. D. Oleschuk, *Mass Spectrom. Rev.*, 2009, **28**, 918–936.
- 7 A. Schmidt, M. Karas and T. Dülcks, *J. Am. Soc. Mass Spectrom.*, 2003, **14**, 492–500.
- 8 M. Gaspari and G. Cuda, *Methods Mol. Biol.*, 2011, **790**, 115–126.
- 9 R. T. Kelly, J. S. Page, R. Zhao, W.-J. Qian, H. M. Mottaz, K. Tang and R. D. Smith, *Anal. Chem.*, 2008, **80**, 143.
- 10 X. Gong, X. Xiong, Y. Zhao, S. Ye and X. Fang, *Anal. Chem.*, 2017, **89**, 7009–7016.
- 11 Z. Takáts, J. M. Wiseman, B. Gologan and R. G. Cooks, *Anal. Chem.*, 2004, **76**, 4050–4058.
- 12 S. Zhang and C. K. Van Pelt, *Expert Rev. Proteomics*, 2004, **1**, 449–468.
- 13 J. L. P. Benesch, B. T. Ruotolo, D. A. Simmons and C. V. Robinson, *Chem. Rev.*, 2007, **107**, 3544–3567.
- 14 J. Liu and L. Konermann, *J. Am. Soc. Mass Spectrom.*, 2011, **22**, 408–417.
- 15 Z. Wei, S. Han, X. Gong, Y. Zhao, C. Yang, S. Zhang and X. Zhang, *Angew. Chem.*, 2013, **125**, 11231–11234.
- 16 M. Matiur Rahman, L. Chen and K. Hiraoka, *Rapid Commun. Mass Spectrom.*, 2013, **27**, 68–74.
- 17 L. Chen, M. Matiur Rahman and K. Hiraoka, *J. Mass Spectrom.*, 2013, **48**, 392–398.
- 18 L. C. Chen, M. K. Mandal and K. Hiraoka, *J. Am. Soc. Mass Spectrom.*, 2011, **22**(12), 2108–2114.
- 19 L. C. Chen, M. K. Mandal and K. Hiraoka, *J. Am. Soc. Mass Spectrom.*, 2011, **22**, 539–544.
- 20 M. M. Rahman, M. K. Mandal, K. Hiraoka and L. C. Chen, *Analyst*, 2013, **138**, 6316–6322.
- 21 M. M. Rahman, K. Hiraoka and L. C. Chen, *Analyst*, 2014, **139**, 610–617.
- 22 L. C. Chen, M. M. Rahman and K. Hiraoka, *Mass Spectrom.*, 2014, **3**, S0024.
- 23 M. M. Rahman and L. C. Chen, *Anal. Chim. Acta*, 2018, **1021**, 78–84.
- 24 P. J. McClory and K. Håkansson, *Anal. Chem.*, 2017, **89**(19), 10188–10193.
- 25 A. P. Bruins, T. R. Covey and J. D. Henion, *Anal. Chem.*, 1987, **59**, 2642–2646.

- 26 Z. Takáts, J. M. Wiseman, B. Gologan and R. G. Cooks, *Anal. Chem.*, 2004, **76**, 4050–4058.
- 27 J. B. Fenn, M. Mann, C. K. Meng, S. F. Wong and C. M. Whitehouse, *Science*, 1989, **246**, 64–71.
- 28 M. G. Ikonomou, A. T. Blades and P. Kebarle, *J. Am. Soc. Mass Spectrom.*, 1991, **2**, 497–505.
- 29 F. M. Wampler, A. T. Blades and P. Kebarle, *J. Am. Soc. Mass Spectrom.*, 1993, **4**, 289–295.
- 30 A. El-Faramawy, K. W. M. Siu and B. A. Thomson, *J. Am. Soc. Mass Spectrom.*, 2005, **16**, 1702–1707.
- 31 G. S. Jackson and C. G. Enke, *Anal. Chem.*, 1999, **71**, 3777–3784.
- 32 M. M. Rahman, T. Jiang, Y. Tang and W. Xu, *Anal. Chim. Acta*, 2018, **1002**, 62–69.
- 33 T. G. Flick, S. I. Merenbloom and E. R. Williams, *J. Am. Soc. Mass Spectrom.*, 2013, **24**, 1654–1662.
- 34 Y. Peng, S. Zhang, F. Wen, X. Ma, C. Yang and X. Zhang, *Anal. Chem.*, 2012, **84**, 3058–3062.
- 35 B. Ji, B. Xia, Y. Gao, F. Ma, L. Ding and Y. Zhou, *Anal. Chem.*, 2016, **88**, 5072–5079.
- 36 N. Talaty, Z. Takáts and R. G. Cooks, *Analyst*, 2005, **130**, 1624–1633.
- 37 J. Sarsby, R. L. Griffiths, A. M. Race, J. Bunch, E. C. Randall, A. J. Creese and H. J. Cooper, *Anal. Chem.*, 2015, **87**, 6794–6800.
- 38 Z. Hall, Y. Chu and J. L. Griffin, *Anal. Chem.*, 2017, **89**, 5161–5170.